

Fine Structure in a High-Resolution Vortex Dissipation Study of $\text{YBa}_2\text{Cu}_3\text{O}_{7-\delta}$

A. L. Barr and J. T. Markert

Department of Physics, University of Texas at Austin, Austin, Texas 78712

(Received 14 December 1995)

Using high- Q double-torsional silicon oscillators vibrating at extremely low amplitude, numerous fine minima and maxima have been observed in the dissipation vs temperature data for certain characteristic fields perpendicular to the c axis in single crystal $\text{YBa}_2\text{Cu}_3\text{O}_{7-\delta}$. These features are mirrored in the frequency shift vs temperature data. An intrinsic pinning model in which the dissipation minima correspond to conditions of commensurability between the interlayer spacing and both the coherence length and Abrikosov lattice spacing is suggested to explain these features. [S0031-9007(96)00725-9]

PACS numbers: 74.60.Ge, 74.25.Ha, 74.72.Bk, 74.80.Dm

Artificially layered Nb/Cu superconductors have shown interesting field-dependent maxima in their magnetization [1]. The layering is used to achieve the condition λ (penetration depth) $> d$ (characteristic dimension) $> \xi$ (coherence length), as is also the case for high- T_c materials, but for the multilayers, the layer spacing merely determines the mass anisotropy, since the coherence length remains relatively long. Shorter coherence length materials such as $\text{YBa}_2\text{Cu}_3\text{O}_{7-\delta}$ (YBCO) should show additional effects [2,3], since the layer spacing is the characteristic dimension of interest. One such effect is due to the phenomena of "intrinsic pinning": For fields parallel to the layers, the vortices prefer to sit between the superconducting CuO_2 planes, since the suppression of the superconducting order parameter between the planes provides a vortex energy minimum there [4]. Such additional pinning can lead to small perturbations in the field and temperature dependencies normally seen in magnetization measurements [5]. Oscillatory tilting of a superconductor in a dc field is one technique for probing the effects of pinning [6,7]. Such studies measure frequency and dissipation changes in the mechanical resonance of the vibrating superconductor. For dissipation studies, such as those done with ac susceptibility or vibrating reeds (or other mechanical oscillators), one normally sees one or two peaks in the dissipation vs temperature data [8,9]. Such peaks arise when flux diffuses through the sample in a characteristic time that matches the inverse of the oscillation frequency. The characteristic time is related to the geometry of the sample and the vortex pinning. For a given field, because the diffusivity changes with the temperature, this condition will be met once during a temperature sweep for each particular diffusion mode, leading to a peak [10]. Typically, one mode dominates; thus, only one dissipation peak is generally seen. It is important to keep the oscillation amplitude small in these studies in order to remain in the linear damping region where local thermally activated depinning events dominate; otherwise, hysteretic damping where the dif-

fusion is nonlinear will set in. In this Letter, we present extremely low amplitude mechanical oscillator data which exhibit numerous unusual maxima and minima in the dissipation data for YBCO as a function of temperature. These additional fine structures, superimposed on the dissipation peaks normally seen, have characteristic properties with regard to field and amplitude. A simple and appealing model based on intrinsic pinning is suggested to explain these features.

As discussed quantitatively for vibrating superconductors by Brandt [11], an ac field applied to a type II superconductor will result in dissipation. The dissipation of an oscillatory system is proportional to $1/Q$, where Q is the usual quality factor. Because the dissipation is dependent on the flux diffusivity which is, in turn, dependent on the activation energy [10], it will be sensitive to various pinning effects throughout the crystal. Besides the dissipation, one may also see changes in the resonant frequency depending on the depth of the pinning potential; i.e., a more strongly pinned vortex which cannot move relative to the crystal will cause an increase in the line tension, and hence restoring force, when the crystal is tilted. The dissipation and resonant frequency are the measured quantities in these oscillator experiments.

Single crystal $\text{YBa}_2\text{Cu}_3\text{O}_{7-\delta}$ crystals were grown from a flux in zirconia crucibles and oxygenated as described previously [12]. A rectangular sample was chosen from the batch. The sample used had an area of $1.38 \times 0.82 \text{ mm}^2$ and mass of $192 \mu\text{g}$. The 10%–90% transition width of the sample was 1 K with the transition onset at 92 K as determined by SQUID magnetometry. The sample was glued 3.5 mm out onto the head of a single crystal silicon double-torsional oscillator which had a frequency of $8 \times 10^3 \text{ Hz}$ and Q of 300 000 at 100 K [13]. The Q 's as a function of temperature were determined from capacitive amplitude measurements. The oscillator was driven sinusoidally across a second capacitive gap, achieving tilt angles between 4×10^{-6} and 5×10^{-8} rad. For this study, a dc field was applied that was nearly

perpendicular to the crystallographic c axis; the oscillator stage was oriented at various small angles (typically 0.5° – 3°) with respect to the field to enable tilt oscillations. Fields between 1 and 8 T and temperatures between 100 and 70 K were employed for most of these studies. Typically, sweeps (requiring many hours, due to the high Q 's employed) were started from above the transition to reduce hysteretic effects from trapped flux of the previous runs.

In Fig. 1, we show dissipation data as a function of temperature for the torsional oscillator and superconducting crystal system. The various curves are sequential in oscillation amplitude, which decreases from top to bottom. This series of runs was taken at the same applied field, 8 T; however, by virtue of the decreasing amplitude, the effective ac field seen by the sample decreases through the series shown. Note that for the ~ 1 mm long crystal the corresponding angular amplitudes are simply related, e.g., 5×10^{-8} rad for the 0.5 Å amplitude. Clearly, the largest amplitude shows the least amount of structure; there is basically a broad peak with a sharper peak near T_c . Mechanical oscillator data taken at much larger amplitudes, $\sim 10^{-3}$ rad, generally show a single smooth peak [14]. As the amplitude drops, the sharper peak becomes more prominent, and, eventually, the broader peak develops structure with several maxima. Other data indicate that these features, and others discussed in this paper, remain in the same relative positions

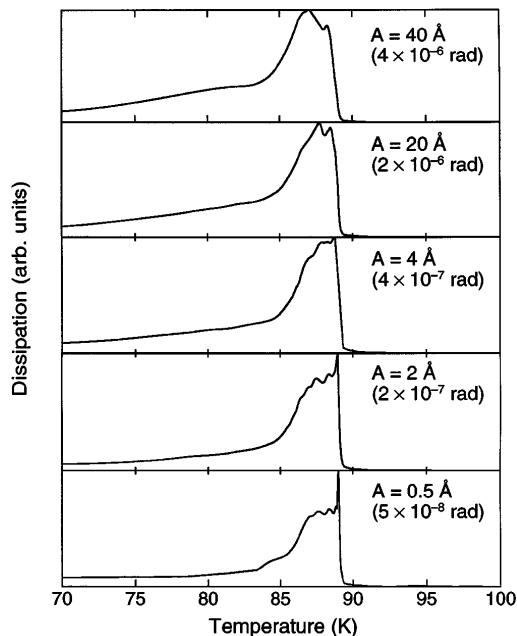


FIG. 1. Dissipation data ($1/Q$) as a function of temperature for a $\text{YBa}_2\text{Cu}_3\text{O}_{7-\delta}$ single crystal with the magnetic field $H = 8$ T applied parallel to the CuO_2 planes. Different frames are for different tilt oscillation amplitudes, given in absolute amplitude (angstroms) and in angular amplitude (radians). Note that the fine structure becomes evident for tilt amplitudes comparable to or less than the superconducting layer spacing.

when the temperature is cycled up or down. Apparently, this fine structure in the dissipation is sensitive to being overdriven. This would be reasonable for any very local pinning potential such as intrinsic pinning, where, for large amplitudes, vortices would be driven across many pinning barriers, washing out any small effects. Note that the majority of the maxima start to become defined between 4 and 20 Å amplitude; this is consistent with an intrinsic pinning picture, where the superconducting layers are separated by $d = 11.8$ Å.

Figure 2 shows the lowest amplitude data for $H = 8$ T. Upon examining the structure of these low amplitude data in more detail, one finds a gradual increase in the minima spacing with decreasing temperature. A simple and appealing possible explanation both for the multiple dissipation maxima and for this spacing is as follows: Using a first-order approximation of a hard core (with semiminor elliptical radius $\xi = \xi_c$) in a sinusoidal intrinsic pinning potential, a vortex would be periodically locked between the planes when the coherence length ξ is approximately equal to some integer n times the superconducting plane spacing d :

$$\xi_n \approx nd. \quad (1)$$

From Ginzburg-Landau theory, the coherence length is a function of temperature [15],

$$\xi(T) = \frac{\xi_0}{(1 - T/T_c)^{1/2}}, \quad (2)$$

where ξ_0 is a parameter [for example, WHHM theory [16,17], ξ_0 is related to the zero-temperature coherence length $\xi(0)$ by $\xi_0 = 1.20\xi(0)$]. Thus the condition for maximum intrinsic pinning, Eq. (1), would be satisfied

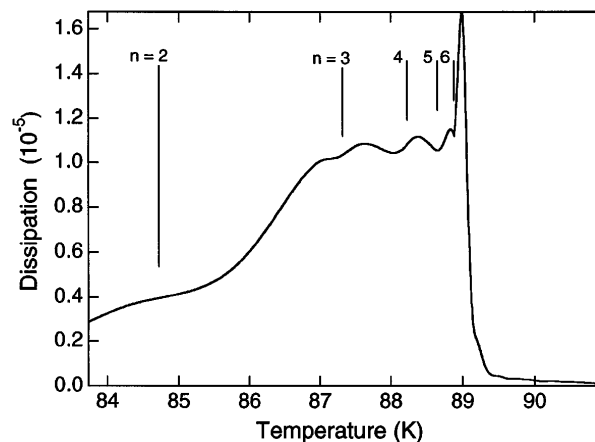


FIG. 2. Smoothed dissipation data ($1/Q$) as a function of temperature at $H = 8$ T for $H||$ planes for the smallest tilt oscillation amplitude studied—approximately 5×10^{-8} rad. Several secondary maxima and minima are resolved. The numbered bars indicate the characteristic temperatures of commensurability between the coherence length and the superconducting layer spacing, reflecting the locations of dissipation minima in an intrinsic pinning model.

at various characteristic temperatures, T_n , obtained by simply inverting Eq. (2):

$$T_n = T_c \left[1 - \left(\frac{\xi_0}{nd} \right)^2 \right]. \quad (3)$$

Using our value of the fitting parameter $\xi_0 = 5.4 \text{ \AA}$, one finds the characteristic temperatures denoted by the vertical bars in Fig. 2, where n runs from 2 to 6. Thus, the minima of the dissipation curve match the intrinsic pinning maxima which correspond to a commensurability of the coherence length and the intrinsic pinning lattice planes.

There is another condition that one might expect if these minima indeed arise from intrinsic pinning. Because the dissipation is a measurement which averages over the whole crystal, having only a few of the vortices located at intrinsic pinning sites is not enough for appreciable effects on dissipation. However, there should exist special fields, for which the anisotropic Abrikosov lattice is commensurate with the interlayer spacing, which allow for coherent vortex trapping across the whole crystal, resulting in the dissipation maxima and minima described above. Commensurate field effects have been seen at much lower temperatures in the cuprates, as well as in multilayer systems [1,5,18]. The special fields for such commensurate behavior are given by [5]

$$H_k = \frac{\sqrt{3} \Phi_0}{2\Gamma d^2 k^2}, \quad (4)$$

where Φ_0 is the flux quantum, Γ is the mass anisotropy parameter [$\Gamma \equiv (m_{\perp}/m_{\parallel})^{1/2}$], and k is an integer starting at 1. The lower inset in Fig. 3 shows the fields for which the vortex lattice is commensurate with the crystallographic lattice spacing (calculated using our magnetically measured value of $\Gamma = 5.8$, which is typical of values obtained by other groups [19,20]). One should see fine structure only near these field values, e.g., 2.1 T (for $k = 10$), 2.6 T, 3.2 T, 4.2 T, 5.8 T, 8.3 T (to $k = 5$, respectively), etc., up to 210 T ($k = 1$). From Figs. 1 and 2, appreciable fine structure was evident near 8 T. From Fig. 3, one also sees fine structure near 6 T, yet the 5 T data do not show fine structure; it is comparatively smooth, as it should be because it is not near a commensurate field. The upper inset of Fig. 3 shows the dissipation as a function of field at the temperature indicated by the arrow in Fig. 3 (a secondary maximum). Although oscillations do appear using this method, they cannot all be directly attributed to commensurability alone. As the field is changed, the dissipation curves also shift down in position relative to the transition temperature in zero field. Any changes in the peak due to commensurability are somewhat obscured by the shifting pattern, especially as the large irreversibility peak moves through this point. For this reason, it is actually more instructive to perform temperature sweeps at different fields so that the field evolution can be decoupled from the pattern shift.

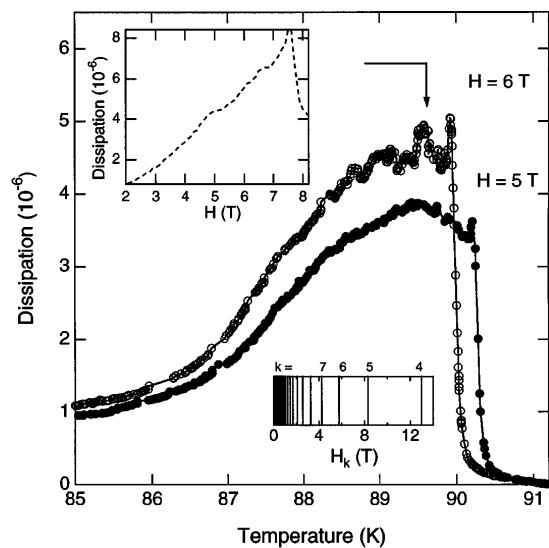


FIG. 3. Dissipation data as a function of temperature for $H = 5$ and 6 T for $H \parallel$ planes. Like the 8 T data, minima are evident at 6 T ; however, they are absent at 5 T . Lower inset: vertical lines indicate the positions of characteristic magnetic fields for which the crystal lattice and vortex lattice are commensurate. Note that magnetic field values of 6 and 8 T are quite close to commensurate fields, while $H = 5 \text{ T}$ falls well between characteristic commensurability fields. Upper inset: dissipation as a function of field at the temperature shown by the arrow.

Finally, we wish to comment on features that accompany the frequency shift which is measured in addition to the dissipation peak. Because of frequency changes rapidly in a small temperature range below T_c (due to the varying penetration depth), any small additional changes in the line tension of a vortex will only appear as very subtle perturbations in the slope of the frequency vs temperature data as seen in Fig. 4(a). The actual changes become more visible by taking the second derivative with respect to temperature. These second derivative data are compared to the corresponding dissipation peak in Fig. 4(b). It is apparent that the oscillations in the curvature of the frequency, i.e., of the vortex stiffness, match the dissipation oscillations discussed above.

In summary, a number of dissipation minima and maxima have been observed for $\text{YBa}_2\text{Cu}_3\text{O}_{7-\delta}$ using high- Q mechanical oscillators; corresponding features are observed in the oscillator frequency shift. This fine structure can be explained within the framework of an intrinsic pinning mechanism. A simple model, in which a hard-core vortex is strongly pinned when the coherence length is an integer multiple of the superconducting plane spacing and also when the Abrikosov lattice is commensurate with the plane spacing, has been suggested to explain the temperature and field behavior, respectively.

Viewed in reverse, such measurements can be likened to a spectroscopy, where the crystal lattice spacing

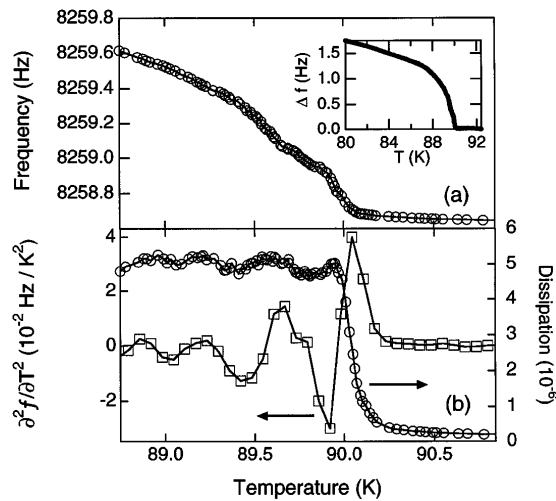


FIG. 4. (a) Mechanical oscillator resonant frequency as a function of temperature for $H = 6$ T, $H \parallel$ planes, for temperatures near T_c , with a tilt oscillation amplitude of several angstroms. On this expanded scale, subtle variations in the frequency shift are barely evident. Inset: Frequency shift over a broader temperature range. (b) The second derivative of the frequency shift of (a) with respect to temperature and the dissipation data, both as a function of temperature. Note that the frequency shift (vortex stiffness) curvature and the dissipation peaks are correlated.

provides the measuring scale to determine the temperature dependence of the superconducting coherence length, as well as, through field-dependent data, the superconducting mass anisotropy.

The authors would like to thank Christopher Wooten, Jeffrey McGuirk, Jonathan Cobb, and Tina Barrett for assistance. This work was supported by the National Science Foundation under Grant No. DMR-9158089 and the Robert A. Welch Foundation under Grant No. F-1191.

- [1] S.H. Brongersma, E. Verweij, N.J. Koeman, D.G. de Groot, R. Griessen, and B.I. Ivlev, *Phys. Rev. Lett.* **71**, 2319 (1993).
- [2] D. Feinberg and A.M. Ettouhami, *Int. J. Mod. Phys.* **B7**, 2085 (1993).
- [3] L. Balents and D.R. Nelson, *Phys. Rev. Lett.* **73**, 2618 (1994).
- [4] D. Feinberg and C. Villard, *Phys. Rev. Lett.* **65**, 919 (1990).
- [5] M. Oussena, P. A. de Groot, R. Gagnon, and L. Taillefer, *Phys. Rev. Lett.* **72**, 3606 (1994).
- [6] S. de Brion, R. Calemczuk, and J.Y. Henry, *Physica (Amsterdam)* **178C**, 225 (1991).
- [7] E.H. Brandt, P. Esquinazi, H. Neckel, and G. Weiss, *Phys. Rev. Lett.* **56**, 89 (1986).
- [8] M. Ziese, P. Esquinazi, and H.F. Braun, *Supercond. Sci. Technol.* **7**, 869 (1994).
- [9] M. Ziese, P. Esquinazi, Y. Kopelevich, and A.B. Sherman, *Physica (Amsterdam)* **224C**, 79 (1994).
- [10] E.H. Brandt, *Phys. Rev. Lett.* **68**, 3769 (1992).
- [11] E.H. Brandt, *Phys. Rev. Lett.* **67**, 2219 (1991).
- [12] R. B. Phelps, P. Akavoor, L.L. Kesmodel, A.L. Barr, J.T. Markert, J. Ma, J. Kelley, and M. Onellion, *Phys. Rev. B.* **50**, 6526 (1994).
- [13] R.N. Kleiman, G.K. Kaminsky, J.D. Reppy, R. Pindak, and D.J. Bishop, *Rev. Sci. Instrum.* **56**, 2088 (1985).
- [14] R.G. Beck, D.E. Farrell, J.P. Rice, D.M. Ginsberg, and V.G. Kogan, *Phys. Rev. Lett.* **68**, 1594 (1992).
- [15] M. Tinkham, *Introduction to Superconductivity* (McGraw-Hill, New York, 1996).
- [16] K. Maki, *Phys. Rev.* **148**, 362 (1966).
- [17] N.R. Werthamer, E. Helfand, and P.C. Hohenberg, *Phys. Rev.* **147**, 295 (1966).
- [18] C. Hunnekes, H.G. Bohn, W. Schilling, and H. Schulz, *Phys. Rev. Lett.* **72**, 2271 (1994).
- [19] U. Welp, W.K. Kwok, G.W. Crabtree, K.G. Vandervoort, and J.Z. Liu, *Phys. Rev. Lett.* **62**, 1908 (1989).
- [20] J.L. Cobb and J.T. Markert, *Physica (Amsterdam)* **226C**, 235 (1994).